JIPE Journal of Infrastructure Planning and Engineering

Journal of Infrastructure Planning and Engineering

Journal homepage: https://ejournal.warmadewa.ac.id/index.php/jipe

Assessing the impact of toll gate construction on land cover alterations with google earth engine

Rendy Akbar[1*], Softy Nuzzela[1], Andi M. Ahsan Mukhlis[1]

[1]*Department of Urban and Regional Planning, Pradita University, Tangerang, 15811, Indonesia*
[*]rendy.akbar@pradita.ac.id

Received on 8 September 2025, accepted on 29 October 2025, published on 31 October 2025

ABSTRACT

In recent years, the Indonesian government has been aggressively pursuing toll road development. Infrastructure projects such as toll roads are known to stimulate economic growth and enhance the mobility of goods and people. This economic growth and increased mobility, in turn, accelerate the process of urbanization. Areas surrounding toll roads, particularly near access points and interchanges, often undergo land use conversion towards functions with higher economic value. Consequently, the presence of a toll road generates a multiplier effect on the surrounding region, encompassing both positive and negative impacts. The Trans-Java Toll Road, a major project connecting the western and eastern ends of Java Island, has been under development for a considerable period. Construction began in 1984, with the connection to Surabaya completed in 2018. Currently, the toll road extends to Probolinggo and is planned to reach Banyuwangi by 2025, spanning a total length of 1,167 km. This study aims to investigate the land cover changes resulting from the construction of the Trans-Java Toll Road, from Merak in the west to Probolinggo in the east of Java. This research employs a quantitative approach, utilizing spatial analysis and descriptive statistics within the Google Earth Engine platform to identify and analyze these land cover changes. This study reveals significant and consistent land cover transformations across the seven analyzed interchanges. Key findings from 1990 to 2020 indicate a universal increase in built-up areas, most substantially observed at the Surabaya interchange, which experienced a 17,681.09 Ha expansion of built-up land. This growth largely occurred at the expense of green areas, which decreased by 15,898.91 Ha in Surabaya and 8,102.97 Ha in Semarang. The Tangerang interchange also showed significant urbanization, with a 3,596.00 Ha increase in built-up land. These findings can serve as a crucial reference for anticipating and mitigating the potential negative consequences of future toll road projects, particularly as the government intensifies infrastructure development in regions outside of Java.

Keywords: toll road, mobility of goods and people, urbanization, land use conversion, land cover change

1 Introduction

As a developing nation, Indonesia is actively pursuing various initiatives to enhance its economic growth. One of the primary strategies is the development of infrastructure, with a particular focus on road networks. Road infrastructure is a critical component for the mobility of goods and people, and it serves as a fundamental element supporting economic, social, and cultural activities [1]. The Indonesian government has prioritized the construction of new road infrastructure, including major toll roads, to trigger rapid growth. This includes the development of the Trans-Java Toll Road, which now connects Merak to Probolinggo, as well as projects outside of Java, such as the Trans-Sumatra Toll Road and new toll roads in Kalimantan and Sulawesi. Consequently, the construction of these toll roads is expected to boost economic growth and mobility, thereby accelerating the process of urbanization [2].

Areas surrounding toll roads, especially near interchanges, are prone to land use conversion, shifting towards functions with higher economic value. Transportation and land use are distinct yet intrinsically linked concepts [3]. Historically, road infrastructure development often followed the locations of existing settlements and activity centers. However, contemporary road projects are now major drivers of land use conversion, stimulating new activities in their vicinity. Land cover change around toll gates is highly probable, with agricultural land and open spaces often being converted into built-up areas [4].

Toll roads possess the capability to connect distant regions, and this infrastructure plays a strategic role in regional development, accelerating the mobility of goods and people, and fostering economic growth in the surrounding areas [5]. In the context of toll road development, the extent of converted land can be used to observe changes in land use for residential, commercial, service, and business purposes. These changes are most prominent around the entrance and exit points of toll interchanges [6]. Land cover represents the physical state of the earth's surface, comprising both natural and man-made elements. The presence of a toll road influences land prices, causing them to increase. This appreciation in land value, in turn, accelerates land cover change. Indeed, road infrastructure development is one of the primary causes of land cover transformation [7].

Massive land cover change can lead to significant social, economic, and environmental impacts. Negative environmental consequences include the degradation of land capability and the emergence of the urban heat island (UHI) effect [8]. The transformation of land cover can be interpreted as improvement, degradation, or damage, depending on the perspective of whether one gains or loses from the transition process. However, large-scale land cover change frequently results in significant land degradation[9].

Therefore, the identification of land cover change is crucial for understanding the impacts of toll road construction and for enabling the formulation of proactive measures to address environmental degradation. The use of Google Earth Engine (GEE) is invaluable for identifying such changes [10]. The advantages of GEE lie in its planetary-scale platform, which utilizes millions of servers worldwide and advanced cloud-computing capabilities for large-scale remote sensing analysis [11]. This study is therefore conducted to analyze the land cover changes resulting from the construction of the Trans-Java Toll Road, with a specific focus on the areas surrounding its interchanges from Merak in the west to Probolinggo in the east. While previous research in Indonesia has effectively documented land cover changes resulting from new infrastructure , these studies often focus on a single, localized toll road section or a specific urban area. A comprehensive, long-term analysis that *compares* the impacts across multiple key interchanges along the entire Trans-Java corridor a project developed over several decades remains a significant research gap. This study is therefore conducted to fill this gap. It provides a large-scale, comparative spatial-temporal analysis of land cover changes at seven major interchanges along the Merak to Probolinggo section. By leveraging the planetary-scale, cloud-computing capabilities of Google Earth Engine (GEE), this research moves beyond a localized case study to identify, quantify, and compare systemic patterns of urbanization across Java's primary infrastructure backbone. The findings are intended to provide a more robust, corridor-level evidence base to help anticipate the cumulative negative impacts of similar toll road projects that the government is now actively pursuing in regions outside of Java.

2 Data and Methods

2.1 Study Area

The Trans-Java Toll Road spans 1,167 km and features 19 primary interchanges. Its construction commenced in 1984 and remains an ongoing process. This study focuses on seven major interchanges along the Merak to Probolinggo section of the Trans-Java Toll Road, namely the Merak, Tangerang, Cikampek, Plumbon, Brebes, Semarang, and Surabaya interchanges. The selection of these seven interchanges was based on several key criteria: (1) their strategic role as major regional economic hubs, (2) their representation of distinct geographical areas along the Trans-Java corridor (West, Central, and East Java), and (3) the consistent availability of high-quality, low-cloud-cover Landsat imagery for the entire study period (1990-2020), which is essential for a valid temporal analysis. The construction timeline for the Trans-Java Toll Road is presented in **Table 1**.

Table 1. Inauguration Year of Trans-Java Toll Road Sections

Section	Length (Km)	Inaugurati on Year
Tangerang - Merak Toll Road	72.45	1984
Jakarta - Tangerang Toll Road	27	1984
Jakarta - Cikampek Toll Road	73	1988
Cikopo - Palimanan Toll Road	116	2015
Palimanan - Kanci Toll Road	26	1998
Kanci - Pejagan Toll Road	35	2010
Pejagan - Pemalang Toll Road	57	2018
Pemalang - Batang Toll Road	39	2018
Semarang - Batang Toll Road	75	2018
Semarang Toll Road	24.75	1983
Semarang - Solo Toll Road	72.64	2018
Solo - Ngawi Toll Road	90	2018
Ngawi - Kertosono Toll Road	87.02	2018
Kertosono - Mojokerto Toll Road	40.50	2018
Surabaya - Mojokerto Toll Road	36.,27	2017
Surabaya - Gempol Toll Road	45	2018
Gempol - Pasuruan Toll Road	34.15	2018
Pasuruan - Probolinggo Toll Road	40	2023
Probolinggo - Banyuwangi Toll Road	164	Under Constructi ons

2.2 Data Collection

The data collection for this study utilized secondary data from Landsat 4, 5, 7, and 8 satellite imagery. The data acquisition process was conducted using the Google Earth Engine platform. Several criteria were applied in the satellite imagery selection process: the recording period was aligned with the construction timeline of the Trans-Java Toll Road from 1980 to 2020, a maximum cloud cover of 20% was specified, and a 5 km buffer was applied around each toll interchange to observe the direct impacts of the toll road's presence. The process continued with the identification of land cover from the acquired satellite imagery.

2.3 Analysis Method

The analysis stages in this study were as follows: delineating the study locations, clipping the Landsat imagery using the delineation polygons, creating land cover samples, performing supervised classification using the Random Forest algorithm, conducting an accuracy assessment by calculating the Overall Accuracy (OA) and Kappa Coefficient, and finally, calculating and interpreting the land cover changes. For further details, please refer to **Figure 1**.

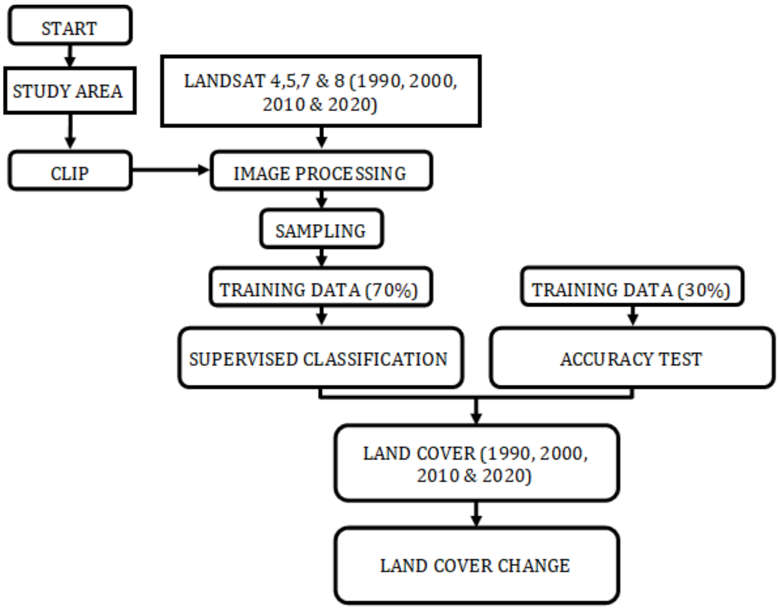

Figure 1. Research Analysis Framework

The tools used in this research analysis were Google Earth Engine (https://code.earthengine.google.com/) and ArcGIS Pro. This study utilized Landsat 7 and 8 satellite imagery from the years 2007, 2012, 2017, and 2022, which were processed, imported, and displayed using Google Earth Engine

The land cover identification method in this study employed the Random Forest (RF) algorithm by executing a script in Google Earth Engine. Random Forest is one of the best-performing ensemble classification algorithms. The RF model is an ensemble learning algorithm, meaning it averages the predictions of many individual trees. Each individual tree is built on a bootstrap sample rather than the original sample, a process known as bootstrap aggregating or "bagging," which reduces overfitting [12].

This Google Earth Engine script performs a supervised land cover classification for the area around the Merak Toll interchange for the year 2020 and can be replicated in other locations and for specified time periods.

1. Image Filtering and Compositing: It starts by creating a function (maskL8) to remove clouds from Landsat 8 imagery. It then searches the Landsat 8 archive for all images taken in 2020, applies the cloud mask to each one, and creates a single, cloud-free composite image by taking the median value of each pixel. This composite is then clipped to the study area (Tol_Merak).
2. Visualization: The script displays the composite image on the map in true color (Red, Green, Blue bands).
3. Training Data Preparation: It merges several predefined geometry objects (e.g., Vegetasi, Badan_Air, etc.) to create a single collection of training samples (training_aoi). It then extracts the spectral data from 7 different bands for these sample points.
4. Classification: A Random Forest classifier is trained using the extracted training data. This trained model is then used to classify every pixel in the composite image, resulting in a land cover map (classified) which is then added to the map with a color palette.

5. Accuracy Assessment: To check how well the classification performed, a separate set of validation points (validation_aoi) is used. The script samples the classified map at these points and compares the map's class with the known class of the validation point. This comparison is summarized in a confusion matrix and an overall accuracy score, which are printed to the console.
6. Area Calculation: The script calculates the total area (in square kilometers) for each land cover class within the study area and prints the results.
7. Export: Finally, the resulting land cover map (classified) is exported to the user's Google Drive for download or further use.

3 Results and Discussion

3.1 Land Cover Identification Analysis

In this study, land cover was classified into four categories: water bodies, green areas, built-up areas, and open land. This land cover classification is based on the Indonesian National Standard (SNI) 7645-1:2014, which was adapted to the specific needs of this research. The resulting land cover maps were generated through an analysis process in Google Earth Engine, which employed the Random Forest (RF) method by executing a script on the platform.

One of the challenges encountered in this study was the interpretation and differentiation of vegetation and grassland cover. This difficulty arose because these two land cover types share similar textural characteristics during the sample selection stage. To mitigate interpretation errors, several classification trials were conducted. The results were then corrected by cross-referencing them with High-Resolution Satellite Imagery (HRSI) from Google Earth. The classification accuracy for vegetation and grasslands can also be enhanced by increasing the number of training samples.

Before analyzing the land cover changes, an accuracy assessment was performed to validate the classification results for each observation year. The Random Forest classifier's performance was evaluated using a confusion matrix, calculating the Overall Accuracy (OA) and the Kappa Coefficient, as mentioned in the methods. The results of this assessment confirmed the reliability of the classification. The classification for the year 2020 achieved an Overall Accuracy of 91.2% and a Kappa Coefficient of 0.89. Similar high-accuracy values were obtained for 1990, 2000, and 2010, indicating that the land cover maps are a robust basis for the subsequent change analysis.

Land cover at the Merak toll interchange consists of water body, green area, open land, and built up area. The largest land cover type in 1990 was open land; in 2000 and 2010, it was water body, and in 2020, it was open land. For further details, please refer to **Table 2** and **Figure 2-5**.

Table 2. Total Area of Land Cover at the Merak Toll Interchange

Year	Area of Land Cover Classes at the Merak Toll Interchange			
	Water Body (Ha)	Green Area (Ha)	Open Land (Ha)	Built – Up Area (Ha)
1990	2061.22	1215.03	3381.35	914.11
2000	1960.04	3932.70	225.66	1457.04
2010	1953.38	2475.36	1579.27	1563.70
2020	1943.48	1720.67	2080.67	1826.88

Land cover at the Tangerang toll interchange consists of green area, open land, and built up area. The largest land cover type in 1990 was green area and from 2000 to 2020, the largest land cover area was built-up area. For further details, please refer to **Table 3.**

Table 3. Total Area of Land Cover at the Tangerang Toll Interchange

Year	Area of Land Cover Classes at the Tangerang Toll Interchange			
	Water Body (Ha)	Green Area (Ha)	Open Land (Ha)	Built – Up Area (Ha)
1990		3354.21	3059.04	1187.43
2000		2185.39	2590.89	2824.39
2010		1934.99	1858.63	3807.06
2020		2185.39	2590.89	2824.39

Land cover at the Cikampek toll interchange consists of green area, open land, and built up area. The largest land cover type in 1990 – 2010 was green area and in 2020, it was open land. For further details, please refer to **Table 4.**

Table 4. Total Area of Land Cover at the Cikampek Toll Interchange

Year	Area of Land Cover Classes at the Cikampek Toll Interchange			
	Water Body (Ha)	Green Area (Ha)	Open Land (Ha)	Built – Up Area (Ha)
1990		4852.63	1498.73	1301.23
2000		3363.01	2781.62	1507.96
2010		3803.52	2093.98	1755.09
2020		2375.11	3295.82	1981.66

Land cover at the Plumbon toll interchange consists of green area, open land, and built up area. The largest land cover type in 1990 was open land; in 2000 and 2010 , it was green area; and in 2020, it was open land. For further details, please refer to **Table 5.**

Table 5. Total Area of Land Cover at the Plumbon Toll Interchange

Year	Area of Land Cover Classes at the Plumbon Toll Interchange			
	Water Body (Ha)	Green Area (Ha)	Open Land (Ha)	Built – Up Area (Ha)
1990		3296.70	4123.65	286.80
2000		3782.25	2834.58	1090.33
2010		2832.19	2603.91	2271.05
2020		1612.83	3732.72	2361.60

Land cover at the Brebes toll interchange consists of water body, green area, open land, and built up area. The largest land cover type in 1990 and 2010 was open land; in 2000 and 2020, it was open land. For further details, please refer to **Table 6**.

Table 6. Total Area of Land Cover at the Brebes Toll Interchange

Year	Area of Land Cover Classes at the Brebes Toll Interchange			
	Water Body (Ha)	Green Area (Ha)	Open Land (Ha)	Built – Up Area (Ha)
1990	87.91	4797.13	2611.48	247.23
2000	1224.38	2477.11	2685.50	1356.75
2010	606.79	2835.68	2554.54	1746.73
2020	393.14	1921.98	3425.33	2003.29

Land cover at the Semarang toll interchange consists of water body, green area, open land, and built up area. The largest land cover type in 1990, 2000 and 2010 was green area and in 2020, it was open land. For further details, please refer to **Table 7**.

Table 7. Total Area of Land Cover at the Semarang Toll Interchange

Year	Area of Land Cover Classes at the Semarang Toll Interchange			
	Water Body (Ha)	Green Area (Ha)	Open Land (Ha)	Built – Up Area (Ha)
1990	2037.75	14475.05	7015.50	6667.54
2000	3330.86	9714.80	9446.11	7442.51
2010	2055.22	10167.04	7597.98	8972.82
2020	2584.38	6372.08	12004.99	10375.60

Land cover at the Surabaya toll interchange consists of water body, green area, open land, and built up area. The largest land cover type in 1990 was green area and in 2000, 2010 and 2020, it was built up area. For further details, please refer to **Table 8**.

Table 8. Total Area of Land Cover at the Surabaya Toll Interchange

Year	Area of Land Cover Classes at the Surabaya Toll Interchange			
	Water Body (Ha)	Green Area (Ha)	Open Land (Ha)	Built – Up Area (Ha)
1990	2999.48	25526.35	16311.14	11804.52
2000	2999.48	11042.26	13114.14	21688.63
2010	3827.20	15154.04	16939.00	23552.59
2020	5399.50	9627.44	18061.96	29485.61

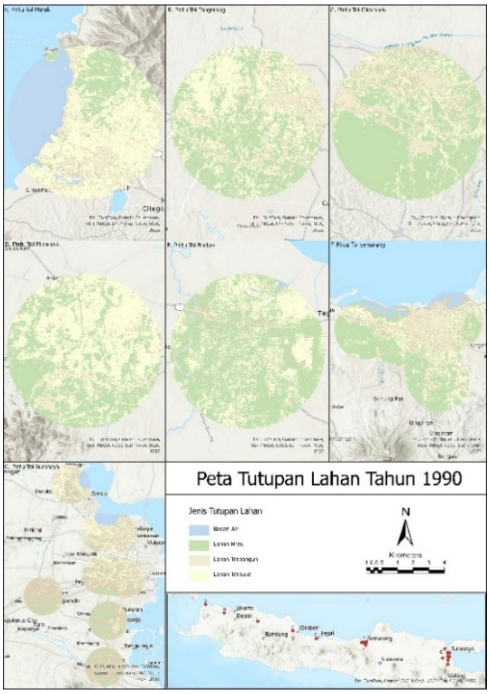

Figure 2. Land Cover Map of 1990

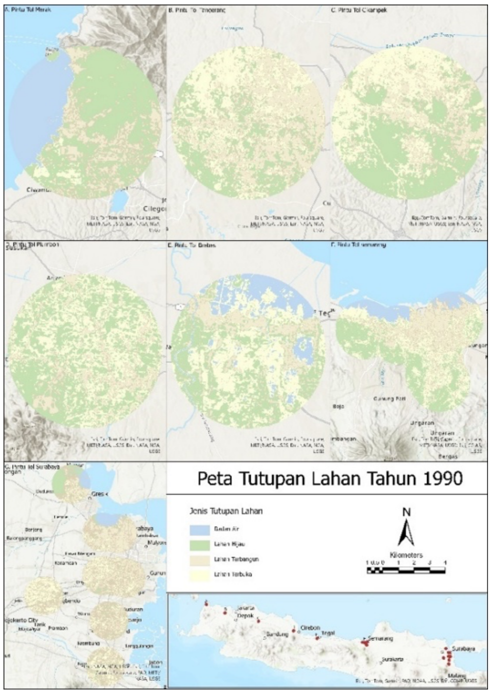

Figure 3. Land Cover Map of 2000

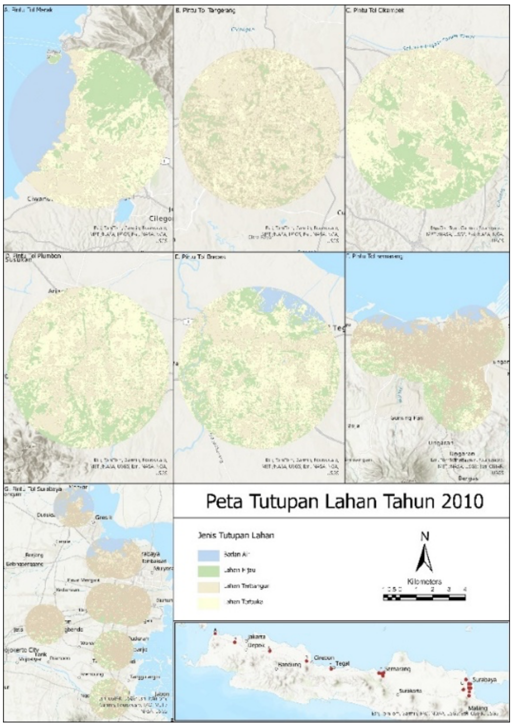

Figure 4. Land Cover Map of 2010

Figure 5. Land Cover Map of 2020

3.2 Land Cover Change Analysis

Land cover change at the Merak Toll Interchange experienced both decreases indicates by a minus sign represents a net decrease (loss) in area for that specific class and increases indicates a net increase (gain) in area. From 1990 to 2020, the land cover class that consistently decreased was water bodies. Meanwhile, green areas and open land experienced periods of both decline and growth. The land cover that consistently increased was built-up area. For further details, please refer to **Table 9.**

Table 9. Land Cover Change at the Merak Toll Interchange

Land Cover Change Periode	Area of Land Cover Change at the Merak Toll Interchange			
	Water Body (Ha)	Green Area (Ha)	Open Land (Ha)	Built – Up Area (Ha)
1990 - 2000	-101.18	2717.68	-3155.70	542.93
1990 - 2010	-107.84	1260.34	-1802.08	649.59
1990 - 2020	-117.74	505.65	-1300.68	912.77
2000 - 2010	-6.66	-1457.34	1353.62	106.66
2000 - 2020	-16.55	-2212.03	1855.02	369.84
2010 - 2020	-9.89	-754.69	501.40	263.18

At the Tangerang Toll Interchange, consistent trends in land cover change were observed. Both green areas and open land experienced a consistent decrease indicates by a minus sign over the study period. Conversely, built-up areas consistently increased indicates a net increase in area. A detailed breakdown of these changes is presented in **Table 10.**

Table 10. Land Cover Change at the Tangerang Toll Interchange

Land Cover Change Periode	Area of Land Cover Change at the Tangerang Toll Interchange			
	Water Body (Ha)	Green Area (Ha)	Water Body (Ha)	Built – Up Area (Ha)
1990 - 2000	-	-1168.82	-468.15	1636.97
1990 - 2010	-	-250.40	-732.27	982.67
1990 - 2020	-	-2301.43	-1294.57	3596.00
2000 - 2010	-	-250.40	-732.27	982.67
2000 - 2020	-	-1132.61	-826.43	1959.04
2010 - 2020	-	-882.21	-94.16	976.37

At the Cikampek Toll Interchange, land cover changes showed distinct patterns. Green areas experienced an almost consistent decrease (indicates by a minus sign) throughout the study period. In contrast, both open land and built-up areas consistently increased (indicates a net increase in area). For a more detailed analysis, please refer to **Table 11.**

Table 11. Land Cover Change at the Cikampek Toll Interchange

Land Cover Change Periode	Area of Land Cover Change at the Cikampek Toll Interchange			
	Water Body (Ha)	Lahan Hijau (Ha)	Water Body (Ha)	Lahan Terbangun (Ha)
1990 - 2000	-	-1489.62	1282.89	206.73
1990 - 2010	-	-1049.11	595.25	453.87
1990 - 2020	-	-2477.53	1797.09	680.43
2000 - 2010	-	440.51	-687.65	247.13
2000 - 2020	-	-987.90	514.20	473.70
2010 - 2020	-	-1428.41	1201.84	226.57

Land cover changes at the Plumbon Toll interchange experienced both decreases indicates by a minus sign and increases indicates a net increase in area. Green areas underwent an almost consistent decrease. In contrast, open land and built-up areas consistently increased. For a more detailed explanation, please see **Table 12.**

Table 12. Land Cover Change at the Plumbon Toll Interchange

Land Cover Change Periode	Area of Land Cover Change at the Plumbon Toll Interchange			
	Water Body (Ha)	Green Area (Ha)	Water Body (Ha)	Built – Up Area (Ha)
1990 - 2000	-	485.54	-1289.07	803.53
1990 - 2010	-	-464.51	-1519.74	1984.25
1990 - 2020	-	-1683.87	-390.93	2074.80
2000 - 2010	-	-950.06	-230.67	1180.73
2000 - 2020	-	-2169.42	898.14	1271.28
2010 - 2020	-	-1219.36	1128.81	90.55

Land cover change at the Brebes Toll Interchange experienced both decreases indicates by a minus sign and increases indicates a net increase in area. The land cover classes that experienced periods of both decline and growth were water bodies, green areas, and open land. The only land cover class that consistently increased was the built-up area. For a more detailed explanation, please see **Table 13.**

Table 13. Land Cover Change at the Brebes Toll Interchange

Land Cover Change Periode	Area of Land Cover Change at the Brebes Toll Interchange			
	Water Body (Ha)	Green Area (Ha)	Water Body (Ha)	Built – Up Area (Ha)
1990 - 2000	1136.47	-2320.01	74.02	1109.52
1990 - 2010	518.88	-1961.44	-56.94	1499.51
1990 - 2020	305.24	-2875.15	813.85	1756.06
2000 - 2010	-617.59	358.57	-130.97	389.98
2000 - 2020	-831.23	-555.14	739.83	646.54
2010 - 2020	-213.64	-913.71	870.79	256.56

Land cover changes at the Semarang Toll interchange involved both decreases indicates by a minus sign and increases indicates a net increase in area. The land cover classes that experienced periods of both decline and growth were water bodies, green areas, and open land. In contrast, the built-up area was the only land cover that consistently increased. For a more detailed explanation, please refer to the **Table 14.**

Table 14. Land Cover Change at the Semarang Toll Interchange

Land Cover Change Periode	Area of Land Cover Change at the Semarang Toll Interchange			
	Water Body (Ha)	Green Area (Ha)	Water Body (Ha)	Built – Up Area (Ha)
1990 - 2000	1293.11	-4760.26	2430.61	774.97
1990 - 2010	17.46	-4308.01	582.48	2305.29
1990 - 2020	546.62	-8102.97	4989.49	3708.07
2000 - 2010	-1275.64	452.25	-1848.13	1530.32
2000 - 2020	-746.48	-3342.72	2558.88	2933.10
2010 - 2020	529.16	-3794.96	4407.01	1402.78

At the Surabaya Toll Interchange, land cover changes included both periods of decreases indicates by a minus sign and increases indicates a net increase in area. The land cover classes of water bodies, green areas, and open land all experienced fluctuations. However, the classes that consistently increased were water bodies and built-up areas. A detailed breakdown of these changes can be seen in **Table 15.**

Table 15. Land Cover Change at the Surabaya Toll Interchange

Land Cover Change Periode	Area of Land Cover Change at the Surabaya Toll Interchange			
	Water Body (Ha)	Green Area (Ha)	Water Body (Ha)	Built – Up Area (Ha)
1990 - 2000	0.00	-14484.09	-3197.01	9884.12
1990 - 2010	827.71	-10372.31	627.86	11748.07
1990 - 2020	2400.02	-15898.91	1750.82	17681.09
2000 - 2010	827.71	4111.77	3824.86	1863.96
2000 - 2020	2400.02	-1414.82	4947.82	7796.98
2010 - 2020	1572.30	-5526.59	1122.96	5933.02

Comparative Analysis Across Interchanges While all seven sites experienced an increase in built-up areas, a cross-location comparison reveals significant variations in the magnitude and nature of these changes. The most dramatic transformation occurred at the Surabaya interchange, where built-up land expanded by 17,681.09 Ha from 1990 to 2020. This massive-scale urbanization, dwarfing all other sites, corresponds to a severe loss of 15,898.91 Ha of green area, highlighting its role as a primary metropolitan hub.

In contrast, the Tangerang and Semarang interchanges also showed substantial, industry- and housing-driven growth, with built-up area increases of 3,596.00 Ha and 3,708.07 Ha, respectively. The Cikampek and Plumbon sites showed more moderate, though consistent, growth. The Merak interchange, despite its strategic port function, showed the most modest increase in built-up area (+912.77 Ha) , suggesting a different development pattern where conversion was more balanced between green areas (-505.65 Ha) and open land (-1300.68 Ha).

3.3 The Impact of Toll Roads on Land Cover Change

Based on the analysis of land cover identification and change, the findings indicate that green areas and open land were the most significantly impacted land cover types. This study's findings identify the Surabaya interchange as the most severely affected location, which lost 15,898.91 Ha of green area, followed by the Semarang interchange, which lost 8,102.97 Ha over the 30-year period. Infrastructure development, such as toll roads, acts as a major driver for this land cover transformation [13]. This phenomenon of land cover change has negative impacts on the surrounding environment [14]. The progressive reduction of open and green areas due to the expansion of built-up land leads to the following environmental, social, and economic impacts [15]:

1. Decreased Land Capability: The extensive replacement of water-absorbent green areas with built-up land—such as the 17,681.09 Ha expansion in Surabaya and 3,708.07 Ha in Semarang. This phenomenon aligns with observations that such massive conversions can trigger hydrological problems and lead to significant land degradation. When green and open areas, which function as water catchment zones, are replaced by impervious materials like asphalt and concrete (built-up areas), the land's natural ability to absorb rainwater decreases drastically. The source identifies this as a primary negative impact. This decrease in capability can trigger hydrological problems, such as increased surface runoff, potentially leading to localized flooding. Furthermore, large-scale conversion directly causes significant land degradation.
2. Urban Heat Island (UHI) Effect: The primary driver for this land conversion is the pursuit of higher economic value. The findings show a consistent increase in built-up areas across all seven sites, from +912.77 Ha in Merak to +17,681.09 Ha in Surabaya. This empirically supports the concept that toll road access fosters economic growth in residential, commercial, and service sectors. The source explicitly states that this land conversion leads to the urban heat island (UHI) effect. This phenomenon occurs because construction materials such as concrete and asphalt absorb and retain more solar heat compared to vegetation and soil. At night, this heat is released back into the atmosphere, causing temperatures in urban areas to be significantly higher than in surrounding rural areas. This has consequences such as increased energy consumption (for air conditioning) and can affect human health.
3. Increased Economic Land Value: The primary driver for this land conversion is the pursuit of higher economic value. The findings show a consistent increase in built-up areas across all seven sites, from +912.77 Ha in Merak to +17,681.09 Ha in Surabaya. This empirically supports the concept that toll road access fosters economic growth in residential, commercial, and service sectors. Infrastructure development like toll roads strategically fosters economic growth in the surrounding regions, including in the residential, commercial, service, and business sectors. This is a positive impact that promotes regional economic growth.
4. Perspective of Improvement vs. Damage: These findings quantify the dual nature of this transformation. From an economic perspective, the growth in built-up areas represents an "improvement". However, from an ecological standpoint, the corresponding loss of productive green and open land—totaling over 26,000 Ha across just the Surabaya and Semarang sites represents significant damage and environmental degradation.

4 Conclusion

This study was conducted to identify and analyze the land cover changes driven by the construction of the Trans-Java Toll Road, utilizing the Google Earth Engine platform for a spatial-temporal analysis. The analysis of seven major toll interchanges reveals significant and consistent patterns of landscape transformation. The most prominent finding is the universal and substantial increase in built-up areas across all study sites. Between 1990 and 2020, the analyzed sites experienced a combined net gain of 30,409.22 Ha of built-up land. This expansion occurred largely at the expense of green areas, which saw a collective net loss of 33,845.51 Ha across the same locations. The impact was most pronounced at the Surabaya interchange, which alone accounted for a 17,681.09 Ha increase in built-up area, corresponding directly to a loss of 15,898.91 Ha of green space.

These findings confirm that large-scale infrastructure projects act as powerful catalysts for urbanization and land use conversion. The observed transformation carries dual implications: while fostering regional economic development through increased land value and new commercial activities , it also leads to significant environmental degradation, including decreased land capability and the Urban

Heat Island (UHI) effect. This research underscores the necessity of using empirical data to anticipate the negative consequences of future development, particularly as the Indonesian government expands infrastructure projects to other islands like Sumatra and Kalimantan.

The methodology employed, leveraging Google Earth Engine and the Random Forest algorithm, proved to be an effective and efficient approach for monitoring these large-scale changes. Future research could build upon these findings by conducting similar baseline studies in planned development corridors outside of Java to support proactive spatial planning. Further studies could also explore the specific socio-economic drivers behind the observed changes in greater detail or model future land cover scenarios to better inform sustainable development policies. Ultimately, this study highlights the critical importance of integrating spatial-temporal monitoring into the infrastructure planning process to balance economic growth with environmental sustainability.

References

[1] S. I. Safitri, A. Yudono, and N. Firdausiyah, "Pengaruh Jalan Tol Terhadap Pertumbuhan Ekonomi Kota/Kabupaten Yang Dilalui Jalan Tol Surabaya-Malang," Planning for Urban Region and Environment, vol. 13, no. 3, pp. 183–192, 2024.

[2] E. S. Hartatik, Wasino, and E. Trihatmoko, "Road Transportation Development And Land Use Changes In Semarang City, Central Java, Indonesia," Indonesian Journal of Geography, vol. 54, no. 3, pp. 409–419, 2022, doi: 10.22146/ijg.66195.

[3] P. L. Hadi, T. Wasanta, and W. Santosa, "Land use change due to road construction," in IOP Conference Series: Earth and Environmental Science, vol. 920, 2021, Art. no. 012003, doi: 10.1088/1755-1315/920/1/012003.

[4] M. Aïkous, J. Dubé, C. Brunelle, and M. P. Champagne, "Highway expansion and impacts on land use changes: An event study approach," Transportation Research Part D: Transport and Environment, vol. 119, Art. no. 103730, 2023, doi: 10.1016/j.trd.2023.103730.

[5] R. G. Funderburg, H. Nixon, M. G. Boarnet, and G. Ferguson, "New highways and land use change: results from a quasi-experimental research design," Transportation Research Part A: Policy and Practice, vol. 44, no. 2, pp. 76–98, 2010, doi: 10.1016/j.tra.2009.11.003.

[6] M. Schonlau and R. Y. Zou, "The random forest algorithm for statistical learning," The Stata Journal, vol. 20, no. 1, pp. 3–29, 2020, doi: 10.1177/1536867X20909688.

[7] W. Salim and U. Faoziyah, "The Effect of Transport Infrastructure on Land-use Change: The Case of Toll Road and High-Speed Railway Development in West Java," J. Reg. City Plann., vol. 33, no. 1, pp. 48–65, 2022, doi: 10.5614/jpwk.2022.33.1.3.

[8] N. Gorelick, M. Hancher, M. Dixon, S. Ilyushchenko, D. Thau, and R. Moore, "Google Earth Engine: Planetary-scale geospatial analysis for everyone," Remote Sensing of Environment, vol. 202, pp. 18–27, 2017, doi: 10.1016/j.rse.2017.06.031.

[9] H. K. Tamiminia et al., "Google Earth Engine for geo-big data applications: A meta-analysis and systematic review," ISPRS Journal of Photogrammetry and Remote Sensing, vol. 164, pp. 152–170, 2020, doi: 10.1016/j.isprsjprs.2020.04.001.

[10] M. Belgiu and L. Drăguţ, "Random Forest in remote sensing: A review of applications and future directions," ISPRS Journal of Photogrammetry and Remote Sensing, vol. 114, pp. 24–31, 2016, doi: 10.1016/j.isprsjprs.2016.01.011.

[11] M. Xu, C. He, Z. Liu, and Y. Dou, "How Did Urban Land Expand in China between 1992 and 2015? A Multi-Scale Landscape Analysis," PLoS One, vol. 11, no. 5, p. e0154839, 2016, doi: 10.1371/journal.pone.0154839.

[12] W. Tesfaye, E. Elias, B. Warkineh, et al., "Modeling of land use and land cover changes using google earth engine and machine learning approach: implications for landscape management," Environ. Syst. Res., vol. 13, Art. no. 31, 2024, doi: 10.1186/s40068-024-00366-3.

[13] R. C. Grecchi, Q. H. J. Gwyn, G. B. Bénié, A. R. Formaggio, and F. C. Fahl, "Land use and land cover changes in the Brazilian Cerrado: A multidisciplinary approach to assess the impacts of agricultural expansion," Applied Geography, vol. 55, pp. 300-312, 2014, doi: 10.1016/j.apgeog.2014.09.014.

[14] S. Alexander, B. Yang, and O. Hussey, "Examining the Land Use and Land Cover Impacts of Highway Capacity Expansions in California Using Remote Sensing Technology," Transp. Res. Rec., vol. 2679, no. 2, pp. 439-449, 2024, doi: 10.1177/03611981241262299.

[15] R. T. T. Forman and L. E. Alexander, "Roads and their major ecological effects," Annu. Rev. Ecol. Evol. Syst., vol. 29, no. 1, pp. 207-231, 1998, doi: 10.1146/annurev.ecolsys.29.1.207.

Appendix

Table Goggle Earth Engine Script

```
// 1. Filter and create a cloud-free image composite
var maskL8 = function(image) {
  var qa = image.select('BQA');
  // Check for the cloud confidence bit and return a mask
  var mask = qa.bitwiseAnd(1 << 4).eq(0);
  return image.updateMask(mask);
};

// Create a median composite for the year 2020, applying the cloud mask
var composite = ee.ImageCollection('LANDSAT/LC08/C01/T1_TOA')
      .filterDate('2020-01-01', '2020-12-31')
      .map(maskL8)
      .median()
      .clip(Tol_Merak); // Clips the composite to the Merak Toll interchange study area
```

```
// 2. Visualize the image
var RGBTrue = composite.select(['B4', 'B3', 'B2']);
var RGBparam = { min: 0, max: 0.3 };
Map.addLayer(RGBTrue, RGBparam, 'TRUE_COLOR_IMAGE');
```

```
// 3. Prepare training data
// Merge all training geometries into a single collection
var training_aoi = Vegetasi.merge(Badan_Air).merge(Lahan_Terbangun)

.merge(Lahan_Kosong).merge(Lahan_Terbuka);

// Define the spectral bands to be used for classification
var bands = ['B1', 'B2', 'B3', 'B4', 'B5', 'B6', 'B7'];

// Extract training samples from the composite image
var training = composite.select(bands).sampleRegions({
  collection: training_aoi,
  properties: ['lc'], // 'lc' is the property storing the land cover class number
  scale: 30
});
```

```
// 4. Train the classifier and classify the image
// Initialize and train a Random Forest classifier
var classifier = ee.Classifier.smileRandomForest(25, 0).train({
  features: training,
  classProperty: 'lc',
  inputProperties: bands
});

// Classify the composite image
var classified = composite.select(bands).classify(classifier);

// Display the classified map
Map.addLayer(classified,
  {min: 0, max: 6, palette: ['darkgreen', 'blue', 'yellow', 'darkblue', 'red', 'orange', 'green']},
  'LandCover');
```

```
// 5. Perform accuracy assessment
// Merge all validation geometries into a single collection
var validation_aoi = Uji_Akurasi_Vegetasi.merge(Uji_BadanAir)
          .merge(Uji_Terbangun).merge(Uji_Tambak)

.merge(Uji_Rumput).merge(Uji_Tanahterbuka)
          .merge(Uji_Sawah);

// Extract validation samples from the classified image
var validation = classified.sampleRegions({
  collection: validation_aoi,
  properties: ['lc'],
  scale: 30,
});
print('Validation Samples:', validation);

// Generate a confusion matrix to assess accuracy
var accuracy = validation.errorMatrix('lc', 'classification');
print('Confusion Matrix:', accuracy);
print('Overall Accuracy:', accuracy.accuracy());
```

```
// 6. Calculate the area of each land cover class
var class_areas = ee.Image.pixelArea().divide(1000 * 1000) // Convert area to sq. km
  .addBands(classified)
  .reduceRegion({
    reducer: ee.Reducer.sum().group({
      groupField: 1,
      groupName: 'code',
    }),
    geometry: Tol_Merak, // The study area
    maxPixels: 500000000,
    scale: 30,
  }).get('groups');

print('Area per Class (in sq. km):', class_areas);
```

```
// 7. Export the result
// Export the classified image to Google Drive
Export.image.toDrive({
  image: classified,
  scale: 30,
  description: 'lc_Tol_Merak_2020',
  region: Tol_Merak
});
```